FO-PID BASED ADAPTIVE POWER OSCILLATION DAMPING CONTROLLER FOR A HYBRID AC/DC MICRO-GRID

Smt K. Firdose Kowser Ahamadia[M.Tech], Assistant Professor, JNTUACEA
Dr M.Rathaiah, Assistant Professor, JNTUACEA.

ABSTRACT

Voltage, frequency, and power oscillations in hybrid AC/DC microgrid increase with load changes due to the parallel operation of many Inductions Motor (IM) drives. Hybrid AC/DC microgrids use an internal DC and AC link to integrate hybrid renewable resources such as wind turbine generators, photovoltaic arrays, and Energy Storage Systems (ESS) with many IMs of various ratings aggregated for dynamic analysis. This paper proposes a Fractional-Order Proportional Integral Derivative Controller(FOPID)controller and compares it to Adaptive Proportional Integral (PI) controller and the results indicate that proposed Adaptive FOPID controller improves oscillatory stability performance in the hybrid AC/DC microgrid.

Index Terms—Power Oscillation Damping, Hybrid AC/DC Micro- Grid, Induction Machine, Low Frequency Oscillations and Fractional Order Proportional Integral Derivative Controller, Adaptive Neuro-Fuzzy Inference System.

I. INTRODUCTION

Hybrid micro-grid combines AC and DC Distributed Generation (DG) systems, ESS systems, and Renewable Energy Sources (RES) into a single system. [2]. They have the potential to improve energy system stability, economics, and sustainability because they Are more controllable and operable than synchronous generators[3]. The hybrid AC/DC micro grid hast wo modes of operation island and grid connected. For hybrid AC/DC microgrids, RES manipulation in island mode is a major challenge to overcome. Due to unusual weather conditions, faults, and continuous load adjustments, the hybrid AC/DC microgrid may also be volatile during the islanded operation mode [4]. According to research[5], [7], microgrid frequency oscillations have been identified as the primary cause of balance issues.

In the power system, commercial, agricultural, and industrial uses account for between 60 and 70 % of total power consumption (depending on the source). Furthermore, the IM of the system is regarded as a dynamic load when operational conditions change (i.e., voltage and frequency). These microgrids are becoming increasingly popular in residential, commercial, and industrial environments. The damping of electrical oscillation shas previously bench own to be affected by IMs [9, 10], and a wide range of IMs with exceptional ratings have been gathered for damping evaluations. The operation of hybrid AC/DC microgrids in various configurations has been examined in several research, using a variety of control techniques [11].

All these methods concentrate on interface microgrid converters to control voltage, frequency, and coordinate load power sharing among connected resources to enhance system power quality. It's important to note that many of these techniques consider pre-determined parameters that affect system performance when operating conditions suddenly change, such as in the case of forced load-shedding. A hybrid isolated AC/DC microgrid is vulnerable to significant voltage fluctuations, especially during load shedding modes in order to avoid instability and unnecessary interruptions.

For a wide range of operational conditions, this paper offers a FOPID controller, which provides dramatically enhanced reaction time. ANFIS was first developed in the early 1990s [11, 12]. There are many advantages of combining neural networks and fuzzy logic in one framework. It uses a fuzzy IF–THEN rule based inference system to approximate nonlinear functions [13]. In reaction to the AC sub grid's nonlinear states machine frequency, the ANFIS controller changes

the gain to reduce oscillations. Using the Inter Linking Converter (ILC), the AC/DC sub grid power flow can be regulated. The following are the results of this investigation:

1. An ANFIS based Power Oscillation Damping(POD) controller damping performance is evaluated under a variety of IM loading conditions, in this paper, the controller's settings are left untouched.
2. The proposed controller's outputs on both sides of the hybrid AC/DC microgrid are verified using many possible parallel operating IM combinations.

MODELLING OF THE HYBRID AC/DC MICROGRID

One such microgrid is depicted in Figure 1. Every cable connecting every Distributed Energy Source (DER) to the Point of Common Coupling (PCC) has a ratio of 0.4 between reactance to resistance(X/R) at low voltage .Both the AC and DC sub-grids are kept at400V,50 Hz and 650 V respectively.

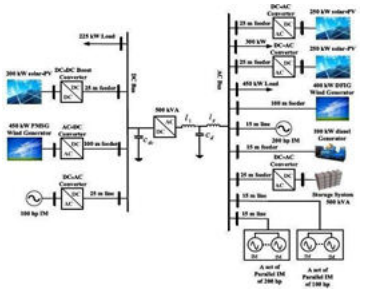

Figure 1 AC/DC hybrid microgrid model

The AC sub-grid is linked to two parallel systems, each rated at 250kW capacity, to increase the overall reliability of solar photovoltaic power. In total, there are 88 strings of seven moduleseach in the 250-kW solar-PV system. Each module's Maximum Power Point(MPP) has voltageand current of 72.9 V and 5.69 A, respectively. The AC sub grid is link ed to a 400kW DoublyFed Induction Generator(DFIG) via a cascaded Power Electronic Converter(PEC).The turbine's maximum wind speed is12m/s. The lithium-ion battery bank has a 500 kVA power supply, and its charge level is kept at 90%. The open-circuit voltage of650 V, and its ampere-hour capacity is 850 Ah. A 500 kVA Inter Linking Converter(ILC) connects the DC and AC subgrades. Islanded operation and power transmission between AC and DC subgrades are both possiblewith the IL Controller. Calculation of power transfer from AC sub grids to DC sub grids and the other way around is done by using current and voltage loops in the ILC controller. Both theDC and AC sub-grids use the DC link and LCL filters capacitor to maintain a constant voltage.The DC sub-grid provides a total of 650 kW of power. The DC sub grid is coupled through a DC- DC boost converter to the Permanent Magnet Synchronous Generator(PMSG) in additionto 200 solar PV system. To obtain a 200-kW system output, 72 parallel strings of seven modulesare required. To connect 225 kW of normal impedance load and the 100 hp IM to the DC sub grid, DC-AC converters are employed. Table 1 shows the results for a wide range of M is loadings.

Table1 IM loading variations

Groups of parallel IM	MODES
4*25hpIM,1*200hpIM, 40*5hpIM	Mode-1
2*50hpIM,1*200hpIM, 20*10hpIM	Mode-2
7*15hpIM,1*200hpIM, 10*20hpIM	Mode-3

CONTROLLER

A. PI Controller

Continuous error can be eliminated using PI control. Integral mode, on the other hand, has an negative impact on the system's response time and overall stability.

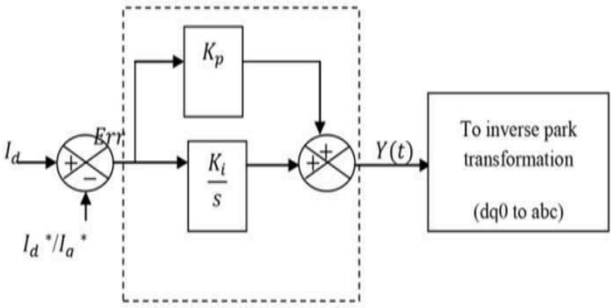

Figure 2 PI controller block diagram

The controller output

$$u(t) = K\,p\,e(t) + Ki\int e(t)\,dt(1)$$

As a result, the response time will not be improved by using a PI controller. This is to be expected because the PI controller doesn't have the ability to predict what the mistake will do soon.

a) When the process is running, there a real too disruptions and noise.

b) One energy store is all that is needed in the procedure.

c) The systemic transport lag is extremely long.

B. FOPID CONTROLLER

FOPID is a branch of mathematics that deals with derivations and integrals. Podlubny proposed the idea of FOPID controllers in 1997. Controlling fractional order systems with a PI controller and an integrator and a differentiator of order, which can be any real numbers, is Muchmore efficient than using the standard controller. In fact, they have five parameters to choosefrom instead of three on standard PI controllers, they theoretically Offer more design flexibility. Controlling dynamical systems described by fractional order mathematical models is one of the key advantages of the FOPID controller. FOPID controllers have another advantage is that they are less sensitive to changes in the parameters of the system they are controlling. This is due to the additional two degrees of freedom that a fractional order control system must better adjust its dynamical characteristics.

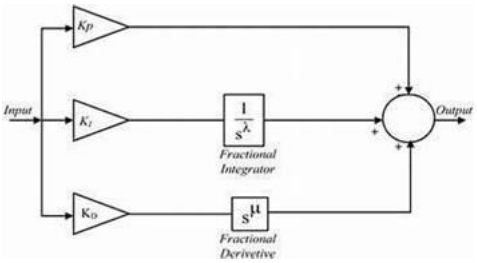

Figure 3 FOPID controller

C. ANFIS POD CONTROLLER

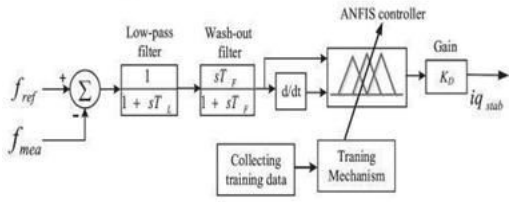

Figure 4 ANFIS POD controller

The external voltage control orphans been developed using an ANFIS based adaptive control system. Based on the variation in AC sub grid frequency, the POD controller provides additional control signals. POD controllers with ANFIS receive frequency deviations from a reference point and predictions of future frequency deviations. An ANFIS uses fuzzy logic and Artificial Neural Network (ANN) to learn and handle massive amounts of data at the same time. As shown in figure

5, ANFIS contains an input layer, three hidden levels, and an output layer.

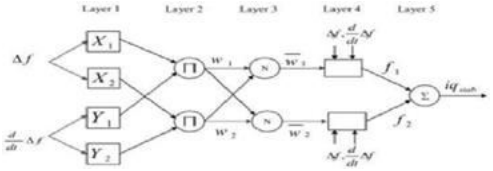

Figure 5 ANFIS architecture ANFIS can be built in three as steps. It employs as

(1) learning paradigm where system data is used as the basis for the learning process

(2) data-driven design, in which the design is based on the system's data and

(3) learning algorithm, which refers to a set of rules for adjusting ANFIS synapse settings, as well as the number of training samples required to train the network. The following are the basic Takagi-Sugeno type rules.

$$if\ (\Delta f\ =\ X1)\ \&\ (\ d\ \Delta f\ =\ y1), then\ f1 = p1\Delta f + q1\ \frac{d\ \Delta f}{dtdt} + r1$$

$$if\ (\Delta f\ =\ X2)\ \&\ (\ d\ \Delta f\ =\ y2), then\ f2 = p2\Delta f + q2\ \frac{d\ \Delta f}{dtdt} + r2 \quad (2)$$

where p1, p2,q1, q2,r1, and r2 are the resulting parameters and X1,X2, and Y1,Y2 are fuzzy sets. Layer 1:Layer 1 is applied to the input variables to create the input variables are represented as fuzzy sets. You can see this by looking at how the nodes in the first layer all have squares for their membership values:

$$Oi\ =\ \mu Xi(\Delta f)$$

$$Oi\ =\ \mu yi(\ \frac{d\ \Delta f}{dt}) \quad (3)$$

The linguistic level is represented by Xi (or Yi), while the node's Membership Function (MF)is represented by Oi. I is the number of the node. Xi is defined in terms of the Gaussian MF(Xi) in the following manner:

$$\mu Xi(\Delta f) = e^{\frac{-1}{2}\frac{(x-c)^2}{\sigma}}\ \mu yi(\ \frac{d}{}$$

$$\Delta f) = e^{\frac{-1}{2}(x-c)^2}$$

(4)

dt σ

where ,c, and σ respectively determine the MF's width and center. Premise parameters are exactly what they sound like.

Layer2:incoming signals from layer1are multiplied by layer2nodes,which are circles. The following is the output of layer2:

$$O2,i = Wi = \mu Xi(\Delta f) * \mu yi(\frac{d}{dt}\Delta f) \quad (5)$$

Wi represents the firing power of each node.

Layer 3:There are as many fuzzy rules as there are layers in layer 3. Its output can be calculated by dividing a node's firing power by the weighted total of all the nodes' firing powers.

$$O3,i = Wi = \frac{Wi}{\sum(W1+W2)} \quad (6)$$

Layer4:Layer4circlenodes have the following output node function

$$O4,i = f1=w1(p1\ \Delta f + q1\ \frac{d}{dt}\Delta f+r1)$$

$$O4,i = f2=w2(p2\Delta f+q2\ \frac{d}{dt}\Delta f+r2) \quad (7)$$

Layer 5:ANFIS' final output is generated by layer 5, which adds all the previous layers 'incoming signals together. The output signal (iqstab) is shown in the following way:

$$O5,i = iqstab = \sum(f1 + f2) \quad (8)$$

Forward and backward passes are necessary for ANFIS controller to establish values for premise and subsequent parameters. Next-generation parameters are evaluated while preexisting parameters remain static; pre-existing parameters are evaluated while following generation parameters remain static in the backward-pass. Training data sets with N inputs can be express ed as follows in terms of error functions for each of the training sets:

$$En = \sum_{p=1}^{m} (Tp, n - Op, n)^2 \quad (9)$$

The pth output vector consists of a reference output vector and an error, as well as pth individual components. As a result, the overall error in measurement is

$$E=\sum_{n=1}^{N} En$$

(10)

We can express the error rate at node (m,i) from(10)as a percentage.

$$\frac{\delta \epsilon n}{\delta o^m} = -2(Ti,n - o^m) \quad (11)$$

Rate of error change in relation to σ is an ANFIS parameter, so

$$\frac{\delta \epsilon n}{\delta \sigma} = \sum_{o \epsilon S} \frac{\delta \epsilon n}{\delta \sigma} \frac{\delta 0}{\delta \sigma}$$

$$\frac{\delta \epsilon n}{\delta \sigma} = \sum_{n=1}^{N} \frac{\delta \epsilon n}{\delta \sigma} \quad (12)$$

In this diagram, S denotes the nodes whose output is dependent on. Thus, the rate of change in

total measured error with respect to time has slowed. Consequently, is denoted by the expression δE δσ. That's how you'd spell the updated generic parameter σ

$$\Delta\sigma = -\beta \cdot \frac{\delta \in}{\delta\sigma}$$

$$\beta = \frac{}{j} \tag{13}$$

$$\sqrt{\frac{\delta \in^2}{(\delta\sigma)\sum\sigma}}$$

Which can be adjusted to speed up convergence by varying both the learning rate(β)and the step size(J).

D. ANFIS POD AND FOPID CONTROLLER

Instead of using PI controller, we replace FOPID controller in the internal current control loops. By using FOPID controller, will improves better than the previous one and dynamic performance of the system improves. FOPID parameter r values give optimal solution.

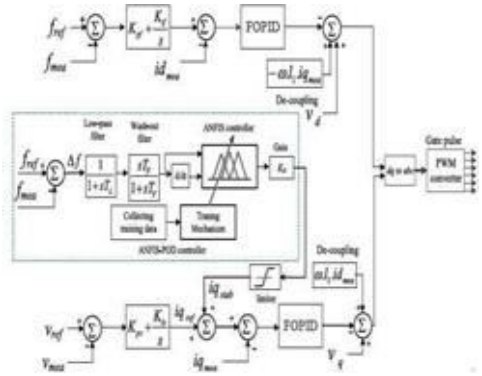

Figure 6 ANFIS based FOPID Controller

II. MATLAB/SIMULATIONRESULTS

Simulink/MATLAB issued to test the AC/DC hybrid microgrid systems performance. For non-linear dynamic simulations, the hybrid AC/DC microgrid was used to account for a variety of known and unknown M loading and turbulence. The simulation block diagram for the hybrid AC/DC micro grid model is shown in figure7. Using simulations, the results of figures8 to10 can be seen.

A) Training mode (load disruptions in the AC sub grid of 26.72 %)
B) Training mode(load disruptions in the DC sub grid of 40.03%)
C) Test mode-1(load disruptions of 26.72 % in the AC sub grid with 2 IM)
D) Testmode-2(load disruptions of 26.72% in the AC sub grid with3 IM)
E) Testmode-3 (load disruptions of40.03% in the DC sub grid with2 IM)
F) Test mode-4(load disruptions of 40.03%in the DC sub grid with 3 IM)
G) Test mode-5(AC sub-grid loses power due toa solar based PV)

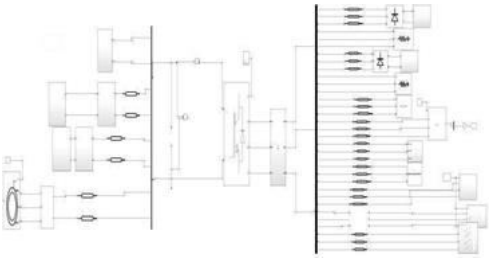

Figure 7 Simulation block diagram for the hybrid AC/DC micro grid model

A. TRAINING MODE (LOAD DISRUPTIONS IN THE AC SUB GRID OF 26.72 %)

As one of three possible IM configurations, the adaptive PI and adaptive FOPID controller was built for mode-1 IM loading (see Table 1). The DC sub grid has 650 kW capacity andtotalgenerationcapacityfortheACsub-gridis1MW.ByusingtheAdaptiveFOPIDcontroller at t=3.0s, we can eliminate grid disturbances caused by AC sub-300kW loads, which we demonstrate and record in this paper. Figures 8(a) and 8(b) show rotor speed of IM and AC sub

grid PCC voltage separately, while Figures 8(c) and 8(d) show the frequency ofACsubgridandoutput.Theseloaddisturbancesarecausingvoltageandfrequencyoscillations in the DC and AC sub grids. Frequency variations in the IM cause rotor speed oscillations, which in turn affect power consumption. Small and large dynamic burdens can have serious consequences when the framework has a high-level penetration of dynamic burden.

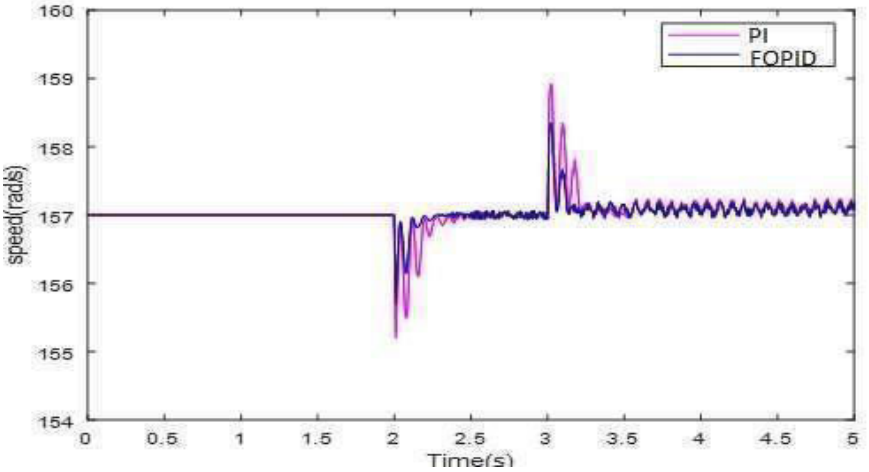

Figure 8(a) Rotor speed of IM

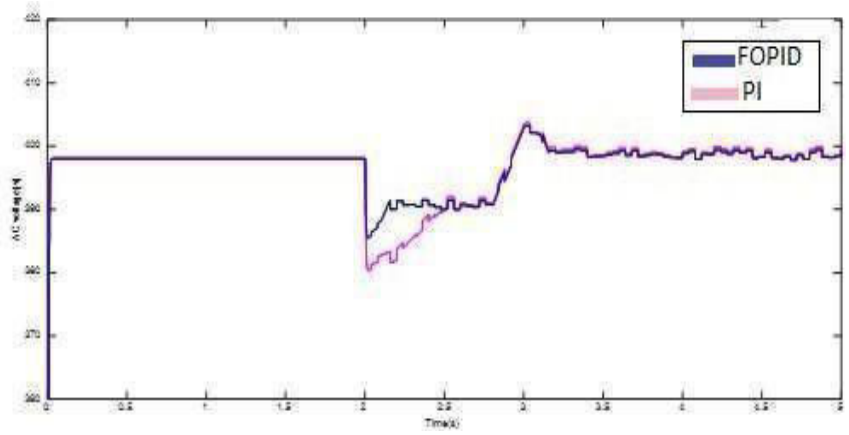

Figure 8 (b) PCC voltage for AC sub grid

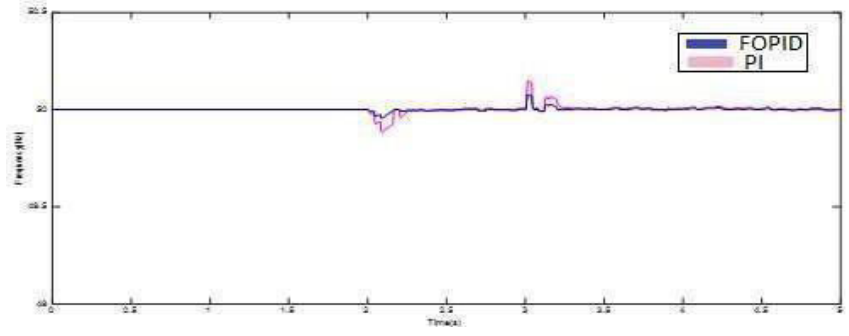

Figure 8(c) Frequency of AC sub grid

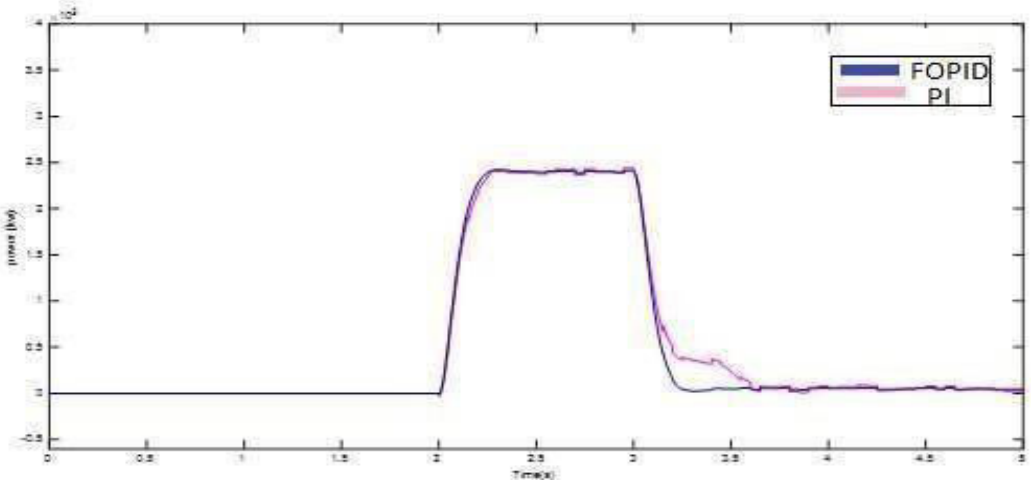

Figure8(d) power injection into AC sub grid

Controller has weakened speed oscillations. Thus, the propose Adaptive FOPID controller gives better damping performance.

B. TRAINING MODE (LOAD DISRUPTIONS IN THE DC SUB GRID OF 40.03%)

There is a similar arrangement of IM loads on this sub-grid. To determine DC sub-adequacy, at time t=2.0s, a 200-kW constant impedance load is coupled to the DC sub-grid and then disconnected at=3.0s.

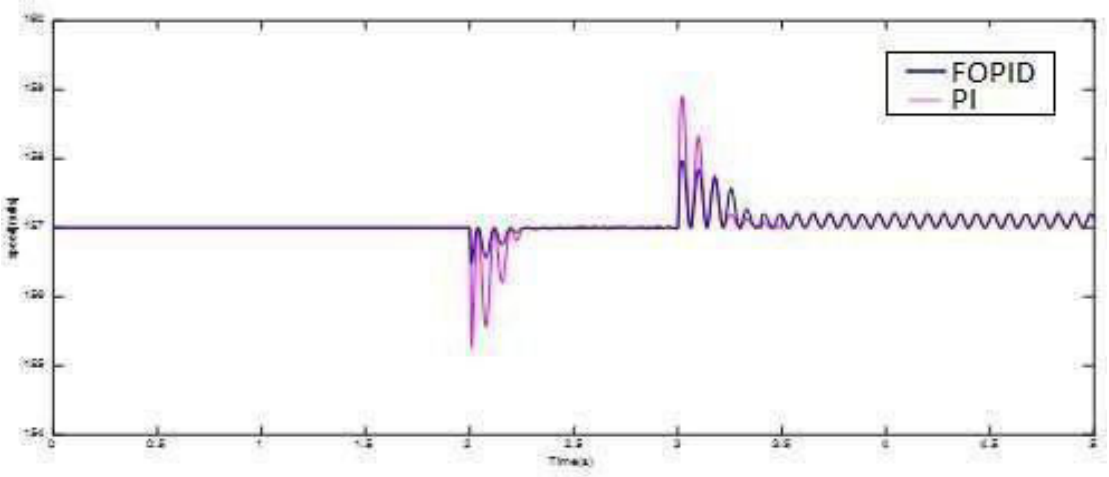

Figure 9(a) Rotor speed of IM

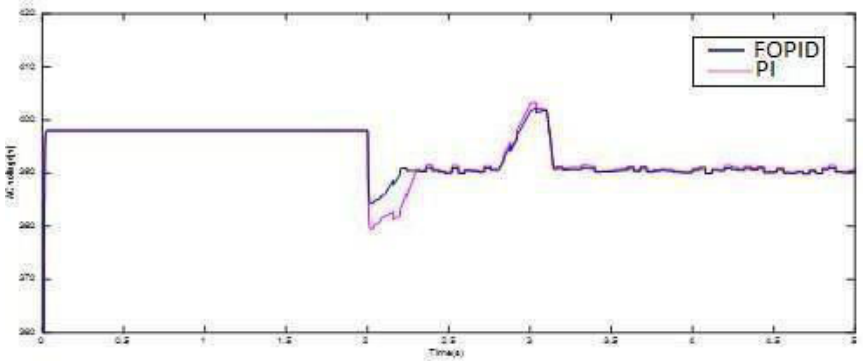

Figure 9(b) PCC voltage for AC sub grid

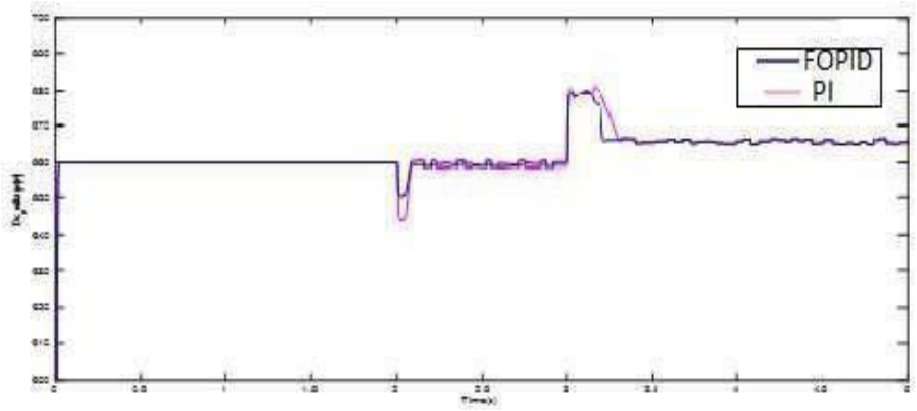

Figure 9(c) PCC voltage for DC sub grid

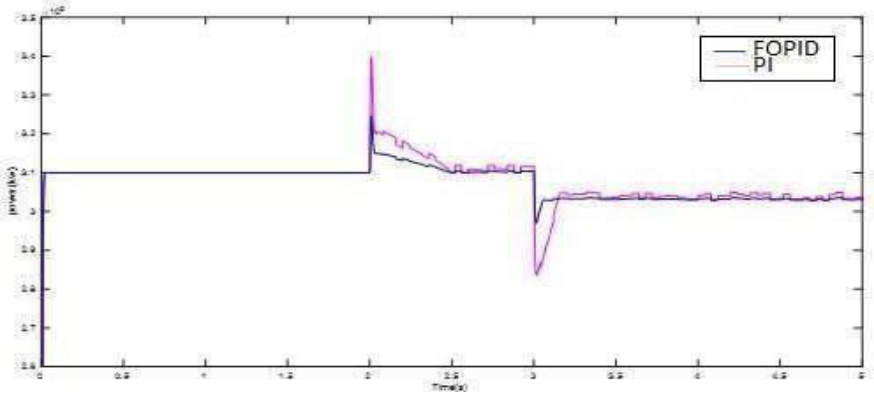

Figure 9(d) power injection into AC sub-grid.

When the AC sub-grid experiences 26.72% load disturbances, as can be seen in figure 9, an AC/DC hybrid microgrid with two IM loads is implemented.

C. TEST MODE-1 (LOAD DISRUPTIONS OF 26.72 % IN THE AC SUB GRID WITH 2 IM)

The IM rotor velocity and AC sub-grid PCC voltage were both depicted in figure10. The voltage and power injection, as shown in figures 10 (c) and 10 (d).When the PI controller is replaced with the FOPID controller, controller provides better response. Both the Power transferred to the AC sub grid, as well as its inadequacy are controlled by an internal current controller, an external voltage and frequency controller in a hybrid AC/DC microgrid. To reduce rotor speed oscillations, an additional signal is added to the controller's outer voltagemanagement loop, as shown in the figure. AC and DC sub grid voltages will be quickly restoredif there is a load disruption with the proposed controller.

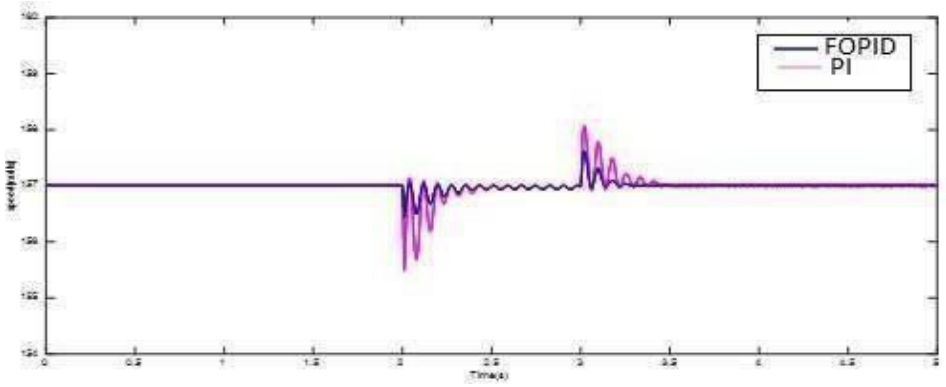

Figure 10(a) Rotor speed of IM

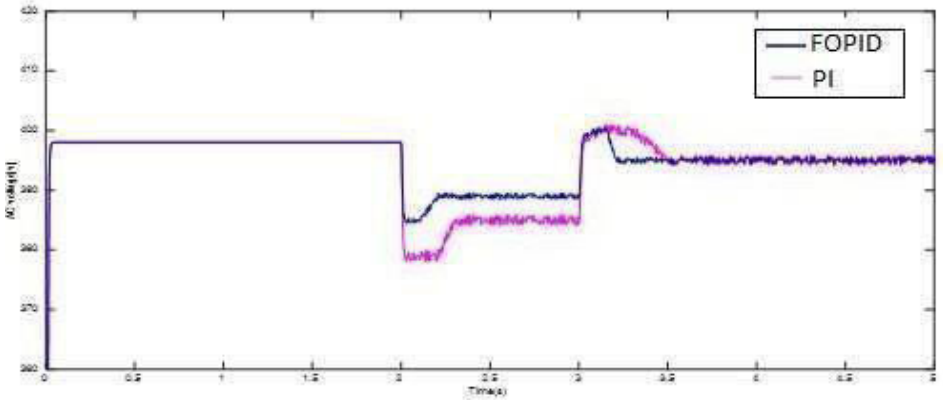

Figure 10(b) PCC voltage for AC sub grid

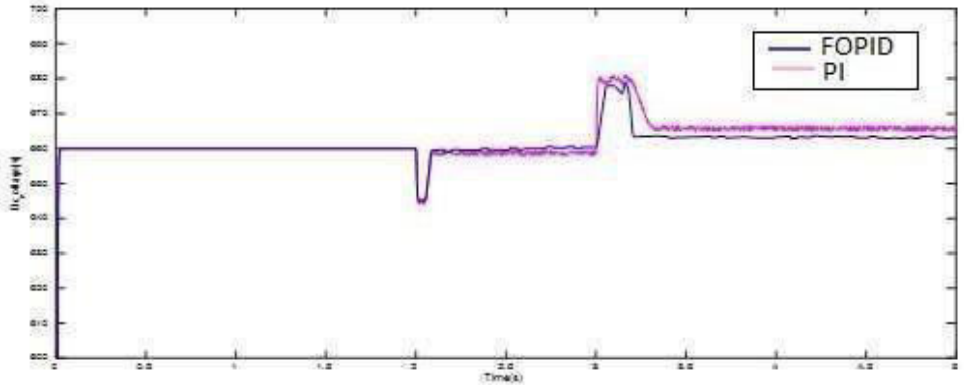

Figure 10(c) PCC voltage for DC sub grid

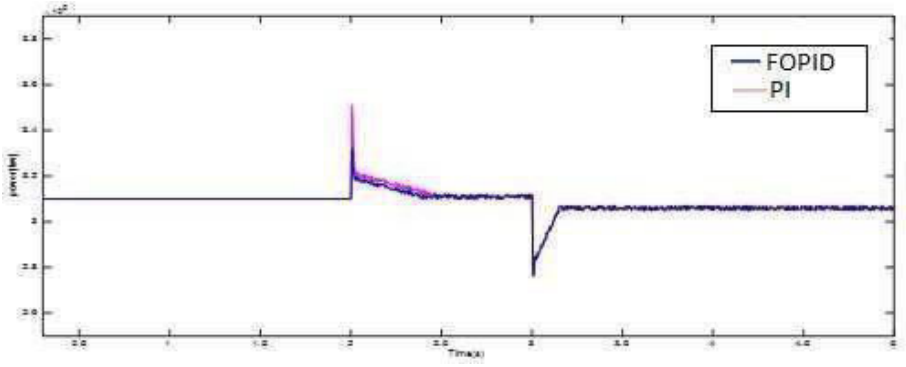

Figure 10(d) power injection into AC sub-grid

D. TEST MODE-2 (LOAD DISRUPTIONS OF 26.72% IN THE AC SUB GRID WITH 3 IM)

Both adaptive FOPID and adaptive PI controller within IM configuration are linked to an AC sub grid. Input time is t=2s, and output time is t=3s. Figure.11 demonstrates how the load disturbance affects both the IM rotational speed and the AC sub-grid voltage. DC sub grid voltage fluctuations and ILC strength injection into the AC sub-grid via ILC are shown infigures11(c)and11(d). As a result of this disturbance, rotor speeds have decreased significantly. The suggested controller has reduced IM rotor speed oscillations for anon trained set of IMs linked to AC sub grid as shown in figure11(a).

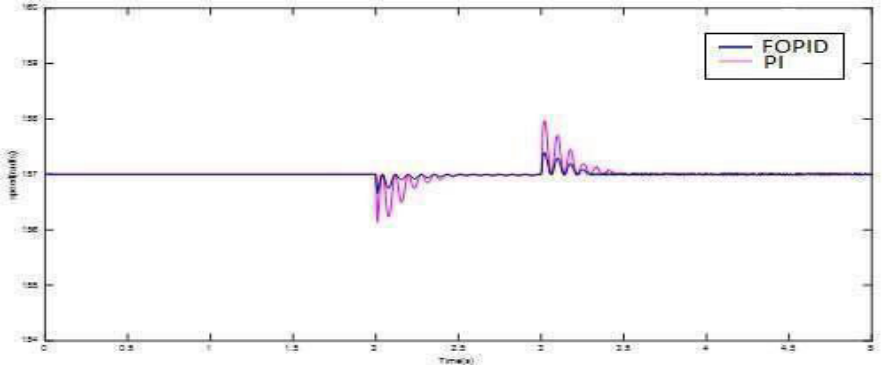

Figure 11(a) Rotor speed of IM

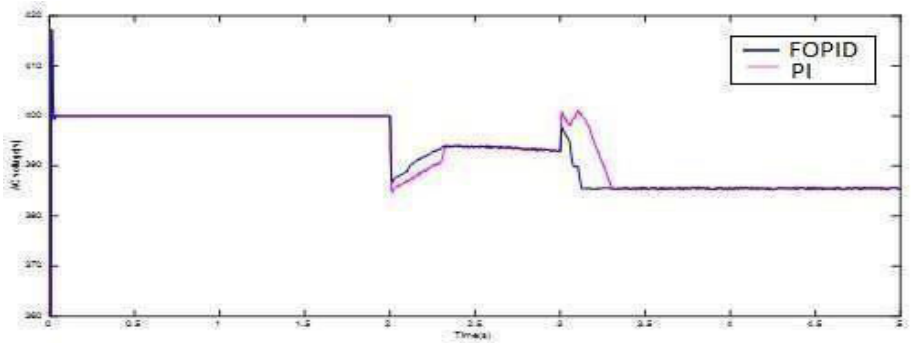

Figure 11(b) PCC voltage for AC sub grid

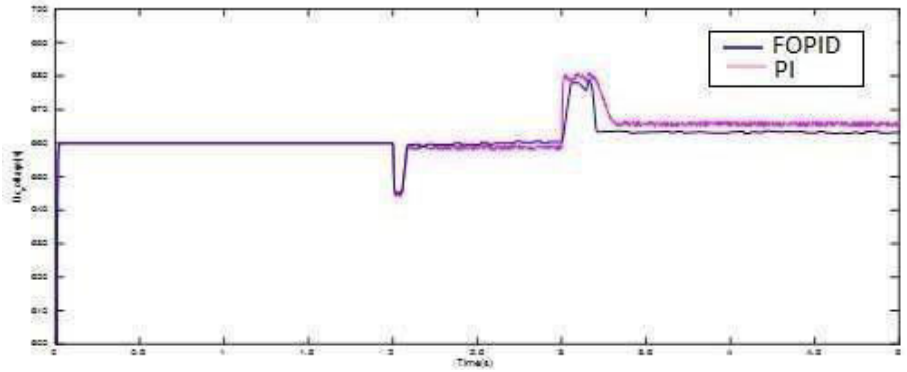

Figure 11(c) PCC voltage for DC sub grid

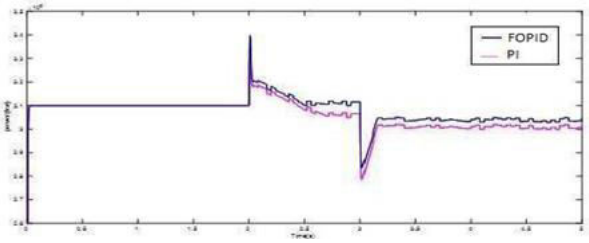

Figure 11(d) The injected power into AC sub-grid

E. TEST MODE-3 (LOAD DISRUPTIONS OF 40.03% IN THE DC SUB GRID WITH 2 IM)

The AC sub-grid is connected to a set of IM loading configurations, referred to as textmode 1. It is proposed that an adaptive FOPID controller be used with a Constant impedance load of 200 kW connected to the DC sub-grid and disconnected (at t=3.0s). This load will be tested for its adaptability. Figures 12(a) and 12(b) show the IM rotor's response to an AC sub-PCC grid voltage. A comparison of DC sub-grid voltage and power injection can be seen infigures12(c) and 12(d).

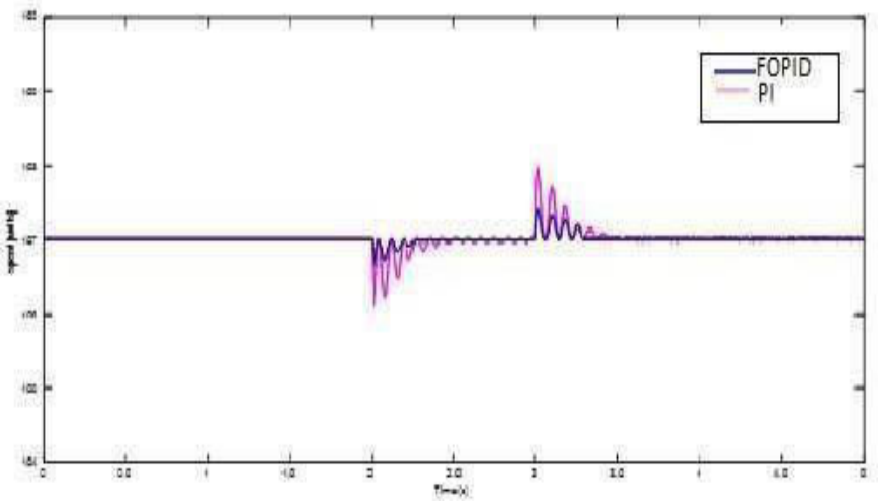

Figure 12(a) Rotor speed of IM

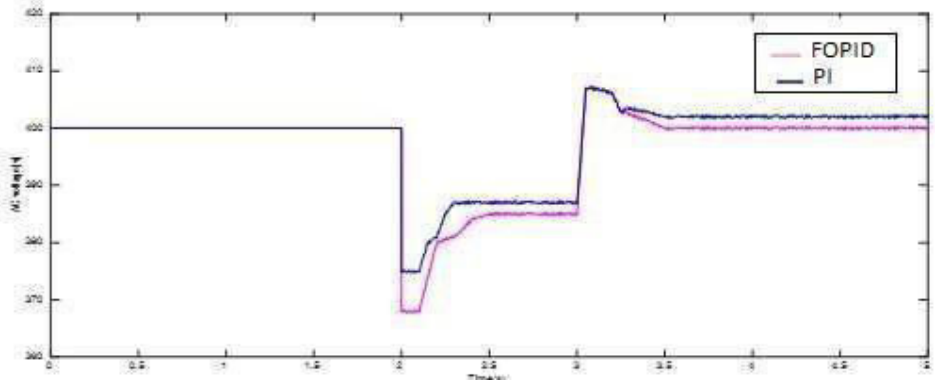

Figure 12(b) PCC voltage for AC sub grid

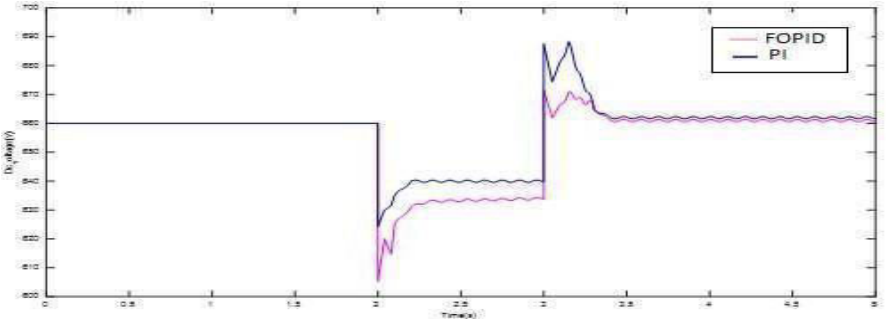

Figure 12(c) PCC voltage for DC sub grid

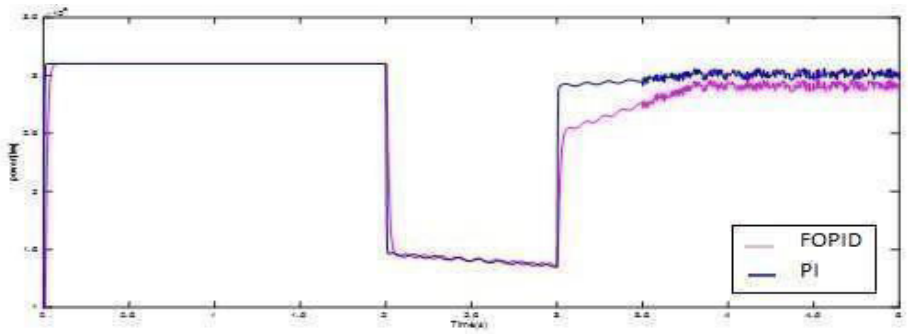

Figure 12(d) The injected power into AC sub grid

F. TEST MODE-4 (LOAD DISRUPTIONS OF 40.03% IN THE DC SUB GRID WITH 3 IM)

In this sub-phase, a substantial load disturbance and an untrained collection of IM loading configurations are applied to see how the adaptive PI and adaptive FOPID controllers handle these two types of disturbances. Even though the total number of IMs that can be loaded has decreased, the IM loading process has not changed in any other way. PCC voltage under step-exchange load infigure13(a) and 13(b) show how the IMrotor performs overall and how well it works with the AC sub-grid under these conditions.

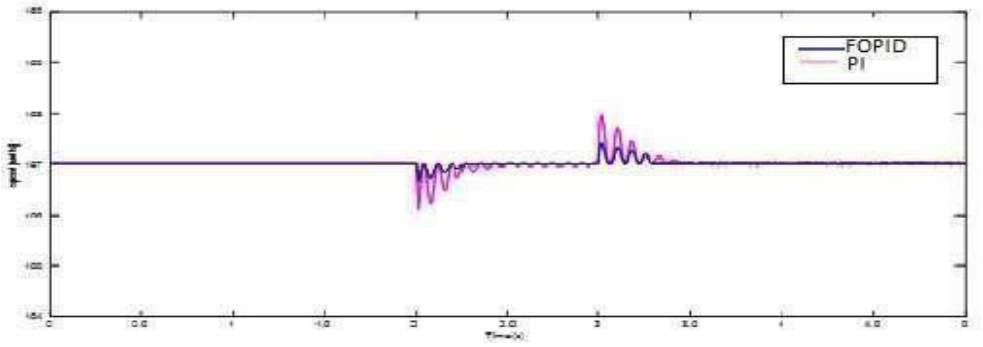

Figure 13(a) Rotor speed of IM

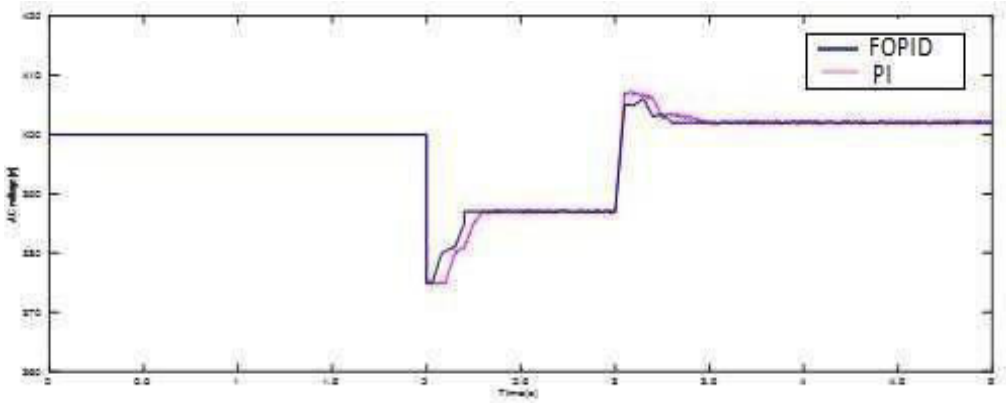

Figure 13(b) PCC voltage for AC sub grid

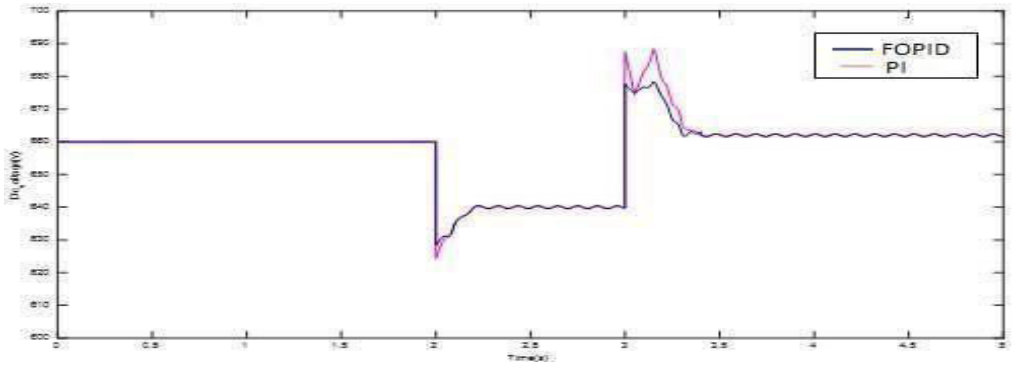

Figure 13 (c)PCC voltage for DC sub grid

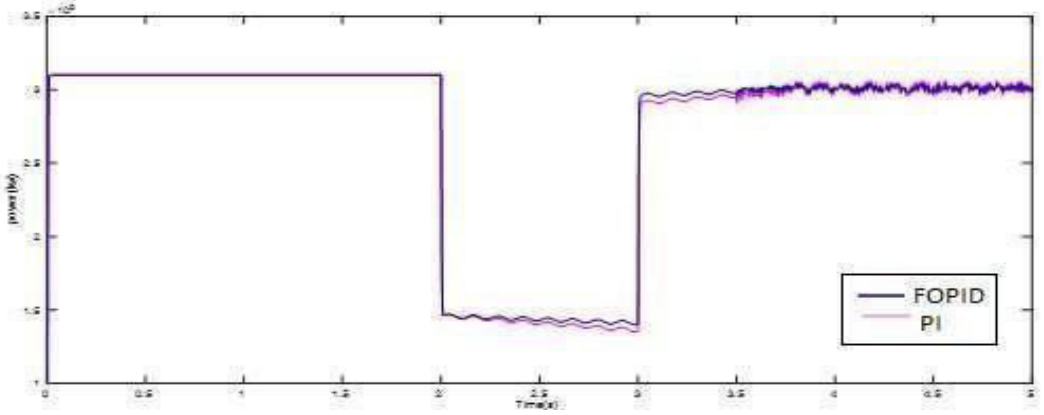

Figure 13(d) The injected power into AC sub grid

G. TEST MODE-5 (AC SUB-GRID LOSES POWER DUE TO SOLAR BASED PV)

The AC sub-grid is connected to a group of IM loading configurations (mode 2). A 250kWsolar-PV system at the AC sub-grid of the hybrid AC/DC microgrid is disconnected at t =2.5sand then reconnected at t=3.5s. The response of rotor speed of IM and the frequency of the AC sub-grid

is shown in figure 14(a) and (b). Load-demand imbalance has been created at the microgrid because of the 250-kW solar- PV system being unplugged from the AC sub grid at time t= 2.5s to 3.5s. As a result, the suggested FOPID successfully works under these conditions.

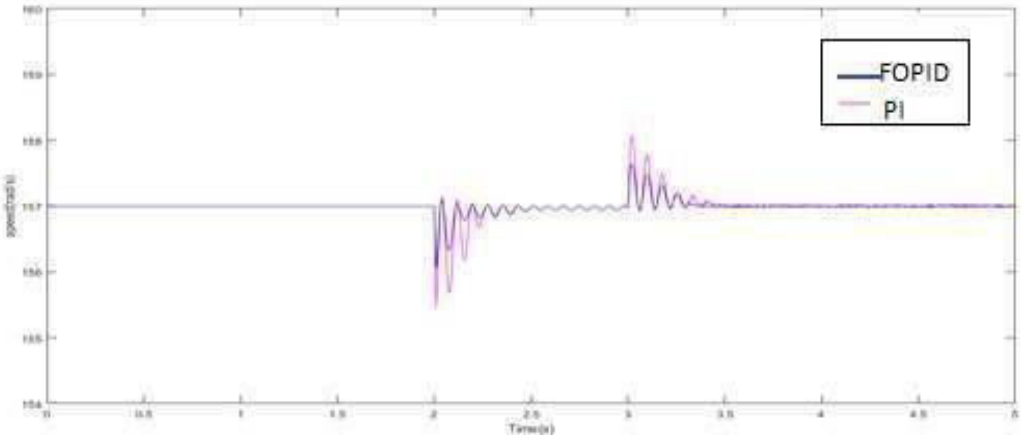

Figure 14(a) Rotor speed of IM

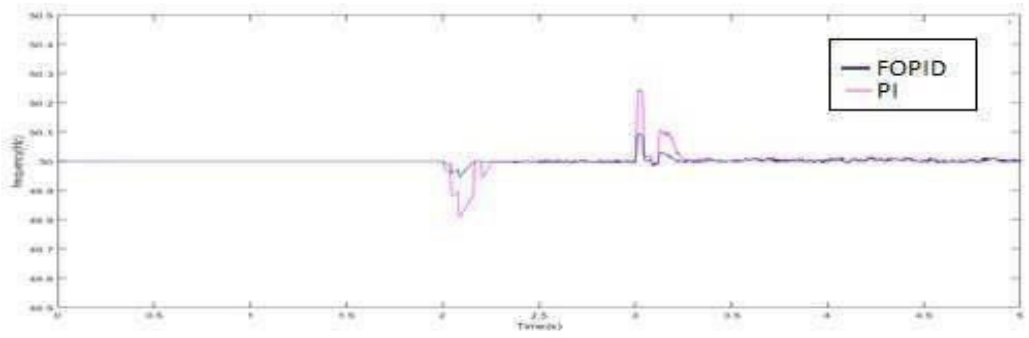

Figure 14(b) AC sub grid frequency.

V.CONCLUSION

An adaptive FOPID controller with various IM loading analyses is proposed in this paper as part of a hybrid AC/DC microgrid. MATLAB/Simulink is used to simulate the AC/DC hybrid microgrid system to verify its performance. The ANFIS POD-based PI and proposed Adaptive FOPID controller significantly improves the AC and DC sub grids' voltage and frequency oscillations, which are caused by any disruption to the hybrid AC/DC micro grid one other side. There was no way to predict the values of parameters accurately with the controller. Based on the frequency deviation and the level of IM loading, the ANFISPOD based PI and FOPID controller automatically adjusts its gain. To test the proposed controller's robustness, various disturbances were applied to the controller. MATLAB/Simulink evaluates the proposed techniques performance under various conditions, and the results show that it performs better.

REFERENCE

[1] Ahmed,Moudud;Vahidnia,Arash;Datta,Manoj;Meegahapola,Lasantha(2020).”AnAdaptive Power Oscillation Damping Controller for a Hybrid AC/DC Micro grid”.IEEEAccess,8(),69495.doi:10.1109/ACCESS.2020.2985978 ,Volume8, 2020.

[2] "Evolutionofmicrogridswithconverter-interfacedgenerations:ChallengesandOpportunities," Int. J. Electr. Power Energy Syst., vol. 109, pp. 160–186, July 2019. M. A.Hossain, H. R.

Pota, M. J. Hossain, and F. Blaabjerg, "Evolution of microgrids with convert-er interface dgenerations: Challenges

[3] "An integrated framework for optimum planning and operation schedule of microgrid under uncertainty," D. R. Prathapaneni and K. P. Detroja," Grids Netw., vol. 19, Sep. 2019,Art.no. 100232. Sustain. Energy, Grids Netw., vol. 19, Sep. 2019, Art. no. 100232.

[4] "Integrating renewable energy in smart grid system: Architecture, virtualization, andanalysis," Sustain. Energy, Grids Netw., vol. 18, Jun. 2019, Art. no. 100226. I. Worighi, A.Maach, A. Hafid, O. Hegazy, and J. Van Mierlo, "Integrating renewable energy in smart gridsystem: Architecture, virtualization, and analysis," Sustain.

[5] "ControlofpowerconvertersinACmicrogrids,"J.Rocabert,A.Luna,F.Blaabjerg,and P.Rodriguez," Nov. 2012, IEEE Trans. PowerElectron., vol. 27, no. 11, pp. 4734–4749.

[6] "Dynamic characteristics of a hybrid microgrid with inverter and noninverter interfacedrenewable energy sources: A case study," in Proc. IEEE Int. Conf. Power Syst. Tech-nol.(POWERCON), Auckland, New Zealand, Oct. 2012, pp. 1–6. A. V. Jayawardena, L. G.Meegahapola,S.Perera,and D. A. Robinson, "

[7] "Improvementofsmallsignalstabilitymarginandtransientresponseininverter-dominated microgrids,"D. K. Dheer, N. Soni,and S. Doolla," Energy,Grids Netw., vol. 5,pp.135–147, Mar.2016.Sus-tain.Energy, GridsNetw., vol.5, pp. 135–147, Mar.2016.

[8] "Modeling,analysis,andtestingofautonomousoperationofaninverter-basedmicrogrid," N. Pogaku, M. Prodanovic, and T. C. Green," Vol. 22, no. 2, pp. 613–625, IEEETrans.Power Electron.,Mar.2007.

[9] "Small-signalstabilityforparallel-connectedin-vertersinstand-aloneACsupplysystems," E. A. A. Coelho, P. C. Cortizo, and P. F. D. Garcia," 533–542, IEEE Trans. Ind.Appl., vol. 38, no. 2, Mar. 2002.

[10] "Small signal stability analysis of a hybrid AC/DC microgrid with static and dynamicloads,"inProc.Australas.UniversitiesPowerEng.Conf.(AUPEC),Melbourne,VIC,Australia, Nov. 2017, pp. 1–6. M. Ahmed, A. Vahidnia, L. Meegahapola, and M. Datta,"Smallsignalstability analysis ofa hybrid AC/DC microgridwithstaticand dynamic